

## DIVISION S-10—WETLAND SOILS

### Quantitative Soil-Landscape Modeling for Estimating the Areal Extent of Hydromorphic Soils

James A. Thompson,\* James C. Bell, and Charles A. Butler

#### ABSTRACT

The spatial distribution of hydromorphic soils across the landscape affects soil survey, broad-scale wetland identification, and ecological studies. The change from upland to wetland is frequently difficult to delineate because it often occurs along a gradual continuum. We have developed a color index, the Profile Darkness Index (PDI), to assist in making these delineations. The PDI is well correlated with the duration of saturated and reducing conditions in specific Mollisol catenas in humid regions of the north-central USA. The objective of this research was to use soil-landscape modeling techniques to relate the variation of PDI to terrain attributes that describe the flow and accumulation of water on hillslopes. Regression models that quantify the relationships between terrain attributes and PDI on a hillslope in west-central Minnesota indicate that variability in slope gradient, profile curvature, and elevation above local depression explained up to 65% of the variability in PDI. These models may be used to estimate the areal extent of hydromorphic soils using terrain attributes derived from a high-resolution (10-m resolution) digital elevation model and to quantify relationships between spatial variability of terrain attributes and of PDI. Knowledge of the terrain attributes that are statistically important according to these models, and their relative effects on PDI (e.g., as slope gradient decreases, PDI increases) may be applied to field-scale delineations of hydric soils.

THE IDENTIFICATION of the areal extent of hydric soils at the landscape scale is essential for regional land-use planning, ecological modeling, and legislative initiatives. Such mapping commonly depends on off-site determinations. Methods currently employed are interpretation of soil survey data that distinguishes between hydric and nonhydric soils, particularly through the use of lists of local, state, or national hydric soils, or evaluation of remotely sensed data such as high-altitude aerial photographs. The inherent uncertainty of soil survey data, including the variability of soil properties within and among soil mapping units (Mader, 1963; Wilding et al., 1964) and the variability of morphological properties that distinguish among soil series (Powel and Springer, 1965; Wilding et al., 1965), makes the use of hydric soils lists problematic. Soil mapping units also may not adequately represent the continuous nature of soil variability by imposing strict boundaries across the landscape.

Remotely sensed data also has limitations because of

difficulties interpreting signal differences due to vegetation or soil variability that may or may not be associated with soil wetness. Stolt and Baker (1995) noted that inventories of the aerial extent of wetlands based on vegetation have significant errors and that the National Wetlands Inventory (NWI) maps, which have been created primarily from remotely sensed data (National Research Council, 1995) to estimate the area of wetlands in the USA, are of unknown accuracy. In Virginia, the NWI maps from two 2.5-min study areas depicted 15.9% or less of the total wetland area identified by a field inventory (Stolt and Baker, 1995). Wetlands in these areas were either obscured by the forest canopy or were too small (0.2–0.6 ha) to be distinguished on the small-scale aerial photography used to generate the NWI maps.

Other concerns with NWI maps are (National Research Council, 1995): (i) depiction of atypical water table conditions at the time of data acquisition, (ii) mapping in level landscapes where wetland boundaries are less abrupt, (iii) and identification of temporarily flooded wetlands where the water table is below the ground surface for most of the year. In areas dominated by Mollisols where surface horizons are dark because of high organic matter contents, differences among hydric and nonhydric soils are not expressed in surface characteristics, further limiting the use of remotely sensed data for off-site determinations.

Field identification and delineation of hydric soils in Mollisol landscapes are similarly problematic because of the presence of the thick, dark surface horizons. Organic ped and particle coatings may mask the presence of commonly observed redoximorphic features used to distinguish soils that formed under seasonally saturated and reducing conditions (Parker et al., 1985). We developed a color index, the PDI, that explains up to 48% of the variability of the duration of saturated and reducing conditions in selected Mollisol landscapes in Minnesota (Thompson and Bell, 1996). This index is also strongly associated with landscape position (e.g., Fig. 5a). The PDI may be a useful intermediary for relating landscape position to hydromorphic properties in Mollisol landscapes.

Attempts to relate topographic variability to soil property variability have been numerous, particularly

J.A. Thompson, Dep. of Agronomy, Univ. of Kentucky, Lexington, KY 40546-0091; J.C. Bell and C.A. Butler, Dep. of Soil, Water, and Climate, Univ. of Minnesota, 439 Borlaug Hall, 1991 Upper Buford Circle, St. Paul, MN 55108-6024. Contribution no. 971250008 from the Minnesota Agric. Exp. Stn., St. Paul, MN. Received 31 July 1996.  
\*Corresponding author (jthompsn@soils.umn.edu).

**Abbreviations:** PDI, Profile Darkness Index; NWI, National Wetland Inventory; DEM, digital elevation model; GPS, global positioning system;  $S$ , slope gradient;  $A_s$ , specific catchment area;  $C_{pro}$ , profile curvature;  $C_{plan}$ , plan curvature; CTI, compound topographic index; SPI, stream power index; STCI, sediment transport capacity index;  $P_d$ , proximity to depression;  $E_d$ , elevation above depression; DPI, depression proximity index; VIF, variance inflation factor.

investigations examining the spatial variations in horizon thickness as a function of topography (e.g., Pennock and de Jong, 1990; Carter and Ciolkosz, 1991; Donald et al., 1993). Regression analyses along two-dimensional transects for individual hillslopes have been used to quantify the relationships between surface topography (distance from summit, slope gradient) and soil properties (particle-size distribution, organic C, cation-exchange capacity, base saturation, depth to carbonates, depth to maximum clay content, and solum thickness) in Iowa (Walker and Ruhe, 1968; Ruhe and Walker, 1968; Kleiss, 1970).

The influence of hillslope morphology and relative landscape position on water movement across a hillslope is particularly important. Mausbach and Richardson (1994) and Khan and Fenton (1994) both discussed the importance of landscape factors in determining the hydrologic regime of a soil and in identifying hydric soil conditions. Bell et al. (1992, 1994a) predicted and mapped soil drainage class across a 7.5-min quadrangle study area using primary and secondary terrain attributes derived from a digital elevation model (DEM), perennial stream and ephemeral surface drainage paths, and soil parent material. For individual watersheds and single hillslopes, terrain analysis techniques have been used to predict surface saturation zones (O'Loughlin, 1986; Moore et al., 1988), zones of erosion and deposition (Moore et al., 1988), and catchment runoff depth and flow velocity (Moore and Grayson, 1991).

Terrain analysis has subsequently been used to empirically model the spatial distribution of soil properties as a function of hydrologically important terrain attributes. Moore et al. (1993) modeled the distribution of A horizon thickness, organic matter content, extractable P, pH, and sand and silt content using selected terrain attributes derived from a DEM. Regression analysis produced coefficients of determination ( $R^2$ ) between A horizon thickness ( $R^2 = 0.51$ ) and depth to carbonates ( $R^2 = 0.44$ ), and by Gessler et al. (1995), who developed statistical models that explained 63% of the variability of A horizon depth and 68% of the variability of solum depth.

Previous spatial modeling efforts using regression techniques often have not incorporated rigorous model validation procedures, such as examination of heteroscedasticity, multicollinearity, and spatial autocorrelation. If present, any of these would reduce the predictive utility of the final model. For example, five of the six models developed by Moore et al. (1993) included either (i) a secondary terrain attribute and a primary terrain attribute of which the secondary terrain attribute is a function, or (ii) two secondary terrain attributes that are functions of the same two primary terrain attributes. These variable pairs are correlated with each other ( $|r| = 0.41$  to  $0.45$  [Moore et al., 1993]), such that multicollinearity may be a problem with these models. In contrast, Odeh et al. (1994) used geostatistical methods such as kriging, co-kriging, and regression kriging to examine soil attribute prediction from DEM-derived terrain attributes. While these geostatistical methods are rigorous, they are also computationally intensive,

involve more estimation of parameters, and require large sample sizes. These requirements make geostatistical methods less useful in broad-scale soil inventory studies.

Our hypothesis was that the spatial patterns of soil attributes can be predicted from spatial patterns of terrain attributes derived from a DEM. We tested this hypothesis using PDI, a soil color index related to the duration of saturated and reducing conditions of humid-region prairie soils (Thompson and Bell, 1996). The ability to directly predict the spatial variability of PDI can then be used to indirectly model the spatial occurrence of hydric soils. Here, PDI is used as an indicator of hydric soil conditions, just as gley soil colors, the presence of redoximorphic features, or other morphological indicators can be used to infer seasonal saturated and reducing conditions. Such a prediction would be useful for assessing, at a landscape scale, the potential location and extent of hydric soils. In this research we addressed spatial autocorrelation of model residuals as a significant concern for spatial prediction of any spatial variable. Detection of spatial autocorrelation is an important aspect of statistical modeling techniques using spatially referenced variables.

## MATERIALS AND METHODS

### Site Description and Sampling

The study site is located on a complex hillslope in west-central Minnesota (Fig. 1). The parent material is calcareous Wisconsinan-age till. The hillslope (Fig. 2) is part of a lateral moraine with approximately 20 m of relief over 400 m; maximum slope gradients are approximately 16%. Morphology of the hillslope is typical, with a level summit, convex shoulder, linear backslope, and concave toeslope (Ruhe, 1975). The backslope is interrupted by a small bench-like feature. The regional drainage pattern is closed in this recently glaciated landscape such that flow collects in a depression at the base of the hillslope with no surface outlet.

Soils of this hillslope are Haploborolls in the upper landscape positions and Endoaquolls in the toeslope and depression. On the south- and west-facing portions of the hillslope, soil samples ( $n = 143$ ) were extracted to a depth of 1 to 2.5 m using a hydraulic probe. Samples were taken at 10- to 20-m intervals along three summit-to-depression transects and four transects along the contour of the hillslope (Fig. 3). The sample locations were registered with a horizontal accuracy of 5 to 10 m using a global positioning system (GPS) receiver (Trimble Navigation, Sunnyvale, CA) with differential correction from a base station at a known location. The transects

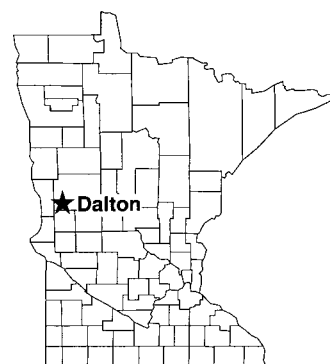


Fig. 1. Location of the Dalton study site in Minnesota.

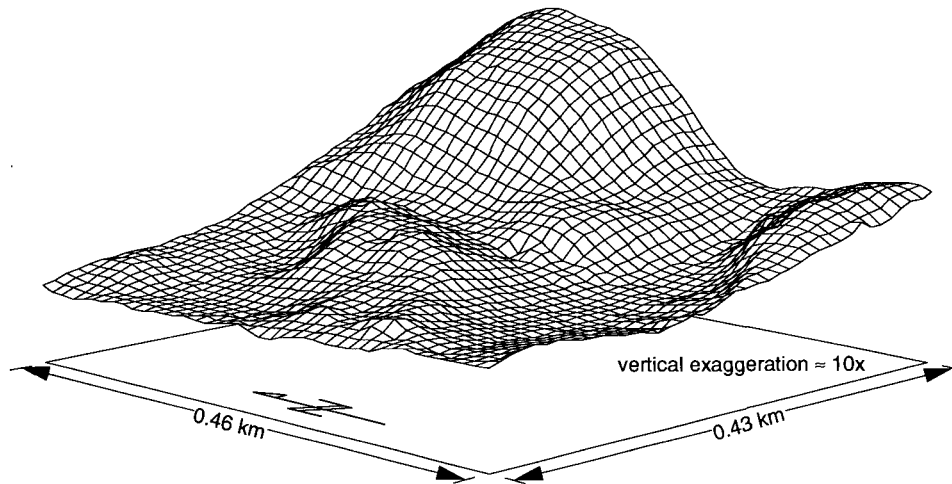


Fig. 2. Perspective diagram of study site topography.

form a three-dimensional catena, with the summit-to-depression transects examining soil variability along the soil drainage gradient from well-drained summit to poorly drained depression. The transects along the contour of the hillslope represent repeated measures at approximately the same location along the drainage gradient.

For each core, the thickness, color, texture, structure, and presence of redoximorphic features of individual horizons (Soil Survey Division Staff, 1993) were recorded (Bell et al., 1994b). From this soil morphologic data, we calculated the value of PDI (Thompson and Bell, 1996):

$$\text{PDI} = \sum_{i=1}^n \frac{\text{A horizon thickness}_i}{(V_i C_i) + 1} \quad [1]$$

where  $V$  is Munsell value,  $C$  is Munsell chroma,  $n$  is the total number of A horizons described, and thickness is measured in centimeters. An A horizon is loosely defined here as any mineral horizon with value  $\leq 3$  and chroma  $\leq 3$ . Subsequently, dark-colored B horizons present in some Mollisols are also included in this index. For each A horizon in the soil profile, the thickness is divided by one plus the product of the Munsell value and chroma. The individual results for all described A horizons are summed to give the final PDI. The PDI increases

as the A horizon(s) become thicker and darker (i.e., value and chroma decrease).

### Terrain Analysis

A 10-m DEM was created from a ground survey using an infrared laser surveyor. Surface elevation measurements were taken along north-south-oriented transects of the entire study site with an approximate 10-m spacing. A universal kriging procedure (Royle et al., 1981) within ARC/INFO (Environmental Systems Research Institute, 1987) was used to interpolate the approximately 1500 irregular grid points to a regular grid DEM of 1778 points (43 by 46).

From this DEM, selected primary terrain attributes (Table 1) were calculated using the Terrain Analysis Programs for the Environmental Sciences-Grid (TAPES-G) program (Moore, 1992). The algorithms used in TAPES-G were described by Moore et al. (1991, 1993, 1994). Drainage direction and drainage area were calculated using a random eight-node algorithm that allows flow dispersion or catchment spreading to occur; slope gradient was calculated using the finite difference algorithm (Moore et al., 1994). Specific catchment area is the area per unit width orthogonal to the flow direction, e.g., square meters per meter (Moore et al., 1991). When calculated from gridded data, specific catchment area is the drainage area divided by the grid-cell size. Additional primary terrain attributes (distance to local depression, elevation above local depression) were calculated from the DEM using algorithms described by Bell et al. (1992) and implemented in Khoros (Khoros Group, 1991). The values for all primary terrain attributes were then extracted for all soil sample locations by

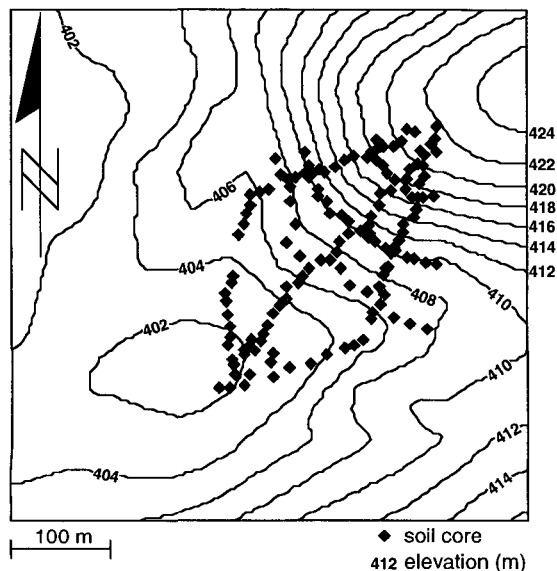


Fig. 3. Contour map of the Dalton study site indicating soil sampling locations.

Table 1. Primary and secondary terrain attributes calculated from a digital elevation model.

Primary terrain attributes	Secondary terrain attributes
Slope gradient, $S$ , %	Compound topographic index, CTI†
Profile curvature, $C_{\text{pro}}$ , $\text{m m}^{-2}$	Stream power index, SPI
Plan curvature, $C_{\text{plan}}$ , $\text{m m}^{-2}$	Sediment transport capacity index, STCI
Tangential curvature, $C_{\text{tan}}$ , $\text{m m}^{-2}$	Depression proximity index, DPI
Specific catchment area, $A_s$ , $\text{m}^2 \text{m}^{-1}$	
Upslope length, $L$ , m	
Distance to local depression, $P_d$ , m	
Elevation above local depression, $E_d$ , m	

† Also referred to as the steady-state wetness index (Moore et al., 1991, 1993, 1994).

assigning the terrain attribute values from the nearest node on the DEM.

Secondary terrain attributes (Table 1) were calculated as linear combinations of two or more primary terrain attributes (Moore et al., 1991, 1993):

$$CTI = \log \left[ \frac{A_s}{S} \right] \quad [2]$$

$$SPI = A_s S \quad [3]$$

$$STCI = \left( \frac{A_s}{22.13} \right)^{0.6} \left( \frac{\sin S'}{0.0896} \right)^{1.3} \quad [4]$$

where  $S'$  is the slope angle in degrees ( $= \arctan S$ ).

An additional secondary terrain attribute, the depression proximity index (DPI) was computed as:

$$DPI = P_d E_d \quad [5]$$

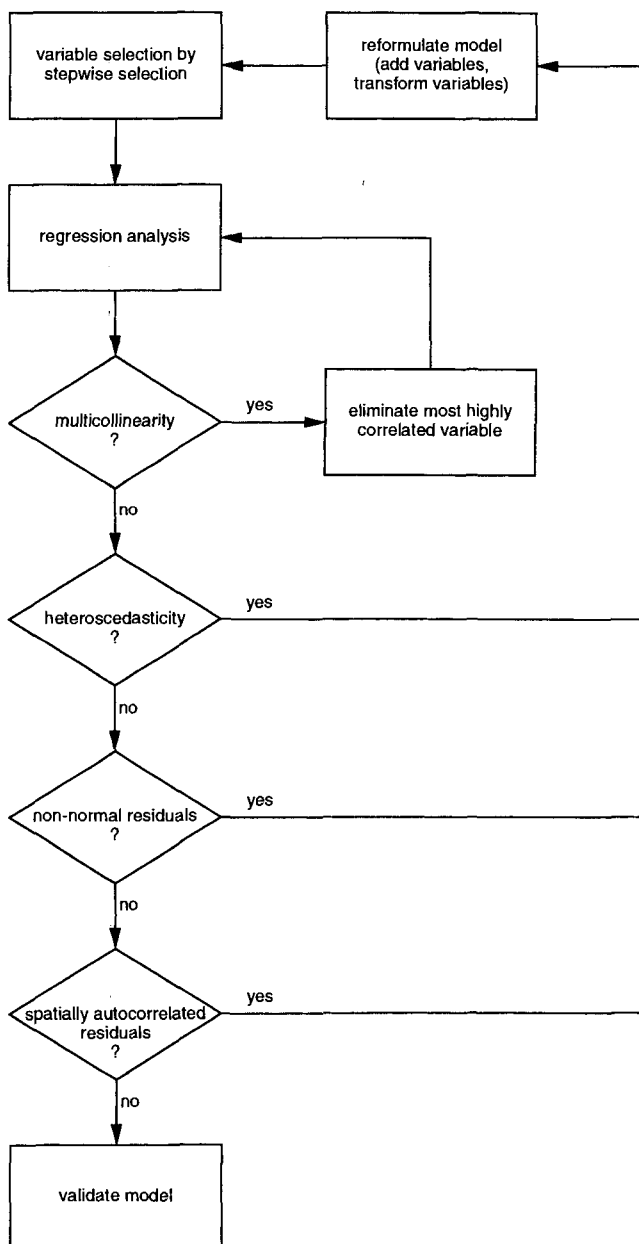


Fig. 4. Flow diagram of model development, verification, and validation procedures.

All of these secondary terrain attributes attempt to quantify some interaction among the primary terrain attributes. The CTI, SPI, and STCI are hydrologically based indexes (Moore et al., 1993), each relating certain aspects of water flow on hillslopes to topography. Similarly, DPI describes the proximity to areas of water accumulation in this closed drainage system. Areas that are both horizontally and vertically closer to the depression are presumably wetter.

### Regression Modeling

Using a split-sample method, we generated and validated multivariate linear models to describe the variability of PDI as a function of terrain attributes (Fig. 4). Statistical modeling was performed using SYSTAT (SYSTAT, 1992). Forward stepwise linear regression (Neter et al., 1989) was used to identify terrain attributes related to PDI using 75% ( $n = 111$ , randomly selected) of the field samples as the training data set. When determining whether a variable will be added (or removed) during each step in the stepwise technique, a level of significance ( $\alpha$ ) is assigned based on a partial  $F$ -test statistic (Neter et al., 1989). This tests the hypothesis that the coefficient of the terrain attribute being considered for addition to the regression model is zero. Choosing a small value for  $\alpha$  increases the probability of omitting a variable that would improve model predictions. This may be considered a more serious error than including a variable that should not be added to the model (Pope and Webster, 1972). An approach for choosing  $\alpha$  is to select a significance value for  $p$  independent variables being considered for inclusion in the model,  $\alpha^*$ , then calculate the model  $\alpha$  as:

$$\alpha = 1 - (1 - \alpha^*)^p \quad [6]$$

With 12 terrain attributes considered for inclusion in our models (Table 1), and an arbitrarily selected  $\alpha^*$  of 0.01, the significance level for this modeling exercise was 0.11.

Another important factor in stepwise regression analysis is the tolerance, which is used to prevent highly correlated independent variables from being included in the model. For a model with  $q$  independent variables ( $q < p$ ), the tolerance is equal to  $1 - R_k^2$ , where  $R_k^2$  is the adjusted coefficient of multiple determination between independent variable  $k$  and the  $q - 1$  other variables currently included in the model. A tolerance of 0.1 was used to minimize the chance of including highly correlated independent variables in the model.

Upon selection of variables in an initial model, the model was tested against the assumptions of linear regression analysis (Neter et al., 1989): no multicollinearity, equal error variance (no heteroscedasticity), and normal and random residuals. Multicollinearity, or high correlations among independent variables, was assessed using the variance inflation factor (Neter et al., 1989, p. 408–410):

$$(VIF)_k = 1 - (1 - R_k^2)^{-1} \quad [7]$$

Multicollinearity may be a problem for an individual  $(VIF)_k$  value  $> 10$  or a mean  $VIF$ ,  $(\overline{VIF})$ , for all independent model variables considerably  $> 1$  (Neter et al., 1989). For this modeling exercise,  $(\overline{VIF}) \geq 2$  was taken as considerably  $> 1$ . Variables with  $(VIF)_k > 10$  were automatically eliminated from the model. If  $(\overline{VIF}) \geq 2$  was calculated, the independent variable most correlated with one or more other independent variables (assessed using a simple correlation matrix) was eliminated.

Model residuals were then examined for the presence of heteroscedasticity (unequal error variance) and normality using a scatter plot of residuals vs. predicted values, histograms, box plots, and normal probability plots (Neter et al., 1989).

**Table 2. Coefficients of correlation ( $r$ ) between selected terrain attributes (untransformed and log transformed) and Profile Darkness Index (PDI) (untransformed and log transformed).**

	$S$	$C_{pro}$	$C_{plan}$	$C_{tan}$	$A_s$	$L$	$P_d$	$E_d$	CTI†	SPI	STCI	DPI
<b>Untransformed terrain attributes</b>												
<b>PDI</b>	−0.50***	0.16	0.13	0.29**	0.34***	0.15	−0.59***	−0.56***	0.32***	0.21*	0.42***	−0.50***
<b>log(PDI + 1)</b>	−0.65***	0.27**	0.29**	0.47***	0.41***	0.27**	−0.68***	−0.71***	0.40***	0.25**	0.50***	−0.64***
<b>Log-transformed terrain attributes</b>												
<b>PDI</b>	−0.55***	−‡	−‡	−‡	0.52***	0.11	−0.54***	−0.60***	0.59***	0.18	0.49***	−0.58***
<b>log(PDI + 1)</b>	−0.68***	−‡	−‡	−‡	0.63***	0.20*	−0.63***	−0.71***	0.72***	0.20*	0.60***	−0.69***

\*, \*\*, \*\*\* Coefficient of correlation significant at the 0.05, 0.01, and 0.001 levels, respectively.

† Antilog of CTI used with “untransformed terrain attributes”.

‡ Log transformation is invalid because of negative values of curvature attributes.

Finally, we examined regression residuals for the presence of spatial autocorrelation (Cliff and Ord, 1981; Odland, 1988). The presence of spatial autocorrelation suggests that there is some systematic variation in the dependent variable for which the model does not account (Odland, 1988). Quantifying the presence of this systematic variation requires a weighting function that describes the interaction between pairs of sample locations. We selected an inverse distance weighting function for this study. A simple algorithm for assessing spatial autocorrelation of regression residuals is given by Jones and Foster (1991). This algorithm was scripted into MacAnova (Oehlert and Bingham, 1993) for calculation of Moran's  $I$  statistic and the expected value of Moran's  $I$ ,  $E(I)$ , based on the independent variables in the model. If  $I$  is significantly greater than  $E(I)$  based on a one-tailed significance test, the hypothesis that the regression residuals are not spatially autocorrelated, i.e., random, is rejected. Because some degree of spatial autocorrelation was evident in all models, we sought to minimize it by considering spatial autocorrelation to be a significant problem above a significance level of 0.001.

After reducing multicollinearity problems, we rejected a model if any of the other model assumptions (heteroscedasticity, non-normal residuals, spatially autocorrelated residuals) were violated. Violation of any of these assumptions indicates that (i) one or more important variables were omitted from the model, or (ii) an incorrect functional form was being used for the model, e.g., linear when the function is actually nonlinear (Odland, 1988). The results of the stepwise regression were only an initial step toward a final model. When one of the regression assumptions was violated, variables were added or removed from the model, and the model again underwent the validation procedure. If adding or removing variables did not remedy the problem, the functional form of the model was altered. In addition to linear models (with and without transformed independent variables), we also examined intrinsically linear models (models that can be transformed to a linear functional form for purposes of regression analysis) (Clark and Hosking, 1986, p. 415–419). Because CTI is defined as the logarithm of the ratio of specific catchment area to slope gradient (Eq. [2]), it was not logarithmically transformed when other independent variables were. Also, when logarithmic transformations of the independent variables were used, the curvature terrain attributes were eliminated from the stepwise regression because curvatures can assume both positive and negative values, and the logarithm of a negative number is undefined.

Models were validated with the remaining 25% ( $n = 32$ , randomly selected) samples using simple regression analysis: the observed PDI values were regressed against those predicted from the application of the individual linear models to the terrain attributes in the validation data set. To assess the models, we used a  $t$ -test to test the hypothesis that the slope

of this regression line equaled 1.0 (Devore and Peck, 1986, p. 459).

## RESULTS AND DISCUSSION

Coefficients of correlation between PDI and the 12 terrain attributes (Table 2) indicate that correlations between PDI and most of the terrain attributes are statistically significant at some level. Several have highly significant ( $P < 0.001$ ) coefficients of correlation with PDI, particularly the depression proximity variables ( $P_d$ ,  $E_d$ , DPI), specific catchment area ( $A_s$ ), slope gradient ( $S$ ), and indexes combining specific catchment area and slope gradient (CTI, STCI). For all terrain attributes, higher coefficients of correlation are found when a logarithmic transformation of PDI is used.

### Regression Modeling

Regression models in which PDI was not logarithmically transformed had low coefficients of multiple determination ( $R^2 < 0.5$ ) and were found to violate one or more of the assumptions of regression analysis. The higher coefficients of correlation between PDI and the terrain attributes when PDI was logarithmically transformed (Table 2), and scatter plots of individual terrain attributes vs. PDI (not shown), suggest that the relationship between PDI and the terrain attributes is nonlinear. Using a logarithmic transformation of PDI incorporates an intrinsically linear functional form:

$$\text{PDI} = ab^x \quad [8]$$

which is modeled linearly after a logarithmic transformation of PDI as:

$$\log(\text{PDI} + 1) = \log a + \log bX \quad [9]$$

where  $X$  is an unspecified terrain attribute. One is added to the value of PDI to avoid taking the logarithm of zero. We examined other intrinsically linear models such as log-log models, polynomial, and reciprocal models, but they are not discussed here because they were found to have low coefficients of multiple determination and/or violated one or more of the regression assumptions.

Two models were identified that (i) satisfied all of the assumptions of regression analysis, (ii) had coefficients of multiple determination  $> 0.5$ , and (iii) had relatively low spatial autocorrelation in the residuals. These models incorporated a combination of the terrain attributes of slope gradient ( $S$ ), profile curvature ( $C_{pro}$ ), plan

**Table 3. Regression equations relating Profile Darkness Index (PDI) to selected terrain attributes and selected descriptive statistics.**

Variable	Model A†	Model B†
Intercept	1.67	1.77
S	-0.055***	-0.051***
$C_{pro}$	0.470**	0.378*
$C_{plan}$	-0.012	—
$E_d$	-0.038***	-0.037***
model $R^2$	0.65	0.64
Moran's $IP$ value‡	0.0013	0.0022
validation $r^2$	0.36	0.40
validation slope§	0.47	0.54
validation $P$ value	0.00049	0.0014

\*, \*\*, \*\*\* Regression coefficient significant at the 0.05, 0.01, and 0.001 levels, respectively.

† Log-transformed PDI, untransformed terrain attributes.

‡ Probability that there is no autocorrelation in the regression residuals.

§ Slope of regression line actual PDI vs. predicted PDI for validation data.

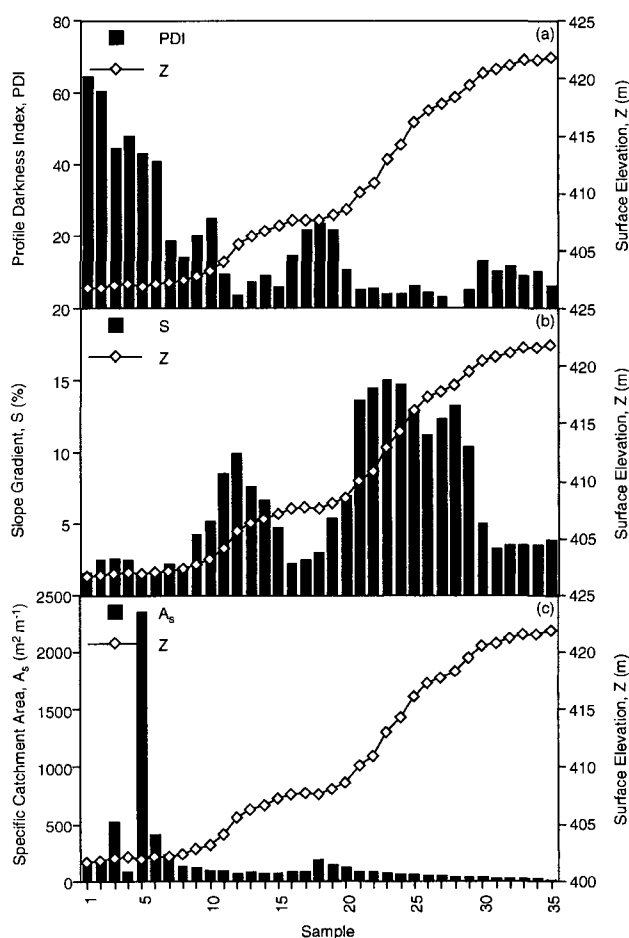
|| Probability that the slope of the validation regression lines = 1.0.

curvature ( $C_{plan}$ ), and elevation above local depression ( $E_d$ ) (Table 3).

The models we developed (Table 3) indicate that as  $S$ ,  $E_d$ , or  $C_{plan}$  decrease, or as  $C_{pro}$  increases, PDI increases. These trends make intuitive sense because decreasing  $S$  and decreasing  $E_d$  are associated with areas of accumulation of both runoff and sediments. Increasing values of  $C_{pro}$  indicate more concave landscape positions. These are also locations where runoff and sediments collect. Conversely, more concave  $C_{plan}$ , indicated by higher positive values, are areas of flow concentration. In higher landscape positions, these locations would have thinner A horizons and lower PDI values.

When compared with a plot of PDI along a transect from summit to depression (Fig. 5a), a plot of  $S$  (Fig. 5b) illustrates why it is such a good predictor of PDI: where slope gradients are low, PDI values are high and where slope gradients are high, PDI values are low. A terrain attribute that is well correlated with PDI (Table 2) but was not included in any of the valid models is specific catchment area ( $A_s$ ). In the depression (Fig. 5c, Samples 1–10) we would expect relatively large values of  $A_s$ . Instead, we find an extremely large  $A_s$  value ( $2350 \text{ m}^2 \text{ m}^{-1}$ ) adjacent to a small value of  $A_s$  ( $77 \text{ m}^2 \text{ m}^{-1}$ ). The remaining  $A_s$  values in the depression are all  $<1500 \text{ m}^2 \text{ m}^{-1}$ . The algorithm for calculating  $A_s$  was developed using open drainage systems, therefore flow is ultimately channelized and an outlet represented by a single cell on the edge of the data. This mental model does not apply in closed drainage systems like the hillslope of our study site because in closed drainage systems there is no such outlet. In the lower landscape positions, flow is probably more dispersive once the lower slope gradients in the toeslope and depression are reached. Seeking a single cell to concentrate all flow is not applicable. Inclusion of  $E_d$  in the model suggests that  $E_d$  is acting as a surrogate for  $A_s$  on this hillslope.

The current algorithm for calculation of  $A_s$ , which does allow flow dispersion, only partitions this flow in upland areas. The partitioning of flow among neighboring cells is a function of the slope to the eight surrounding cells. In lower landscapes, flow is forced to channelize, which is natural in open drainage systems.

**Fig. 5. Transect plots for (a) Profile Darkness Index, PDI; (b) slope gradient,  $S$ ; and (c) specific catchment area,  $A_s$ .**

The algorithm allows the user to set the threshold at which flow dispersion ceases and all flow is routed to a single cell. Even setting an extremely large threshold (greater than the total area covered by the DEM) does not eliminate the requirement for a single outlet cell. In closed drainage systems, channelized flow on the backslope and footslope is again dispersed in the toeslope and depression. It may be possible to identify these dispersing slope positions from the DEM based on relative slope differences among all neighboring cells as well as slope curvatures. Also in closed drainage landscapes it is necessary to eliminate the search for a single outlet cell because in depressional areas water accumulates over the entire broad bottom of the slope.

Application of the two linear models to the validation data produced validation  $r^2$  values of 0.36 and 0.40; the slopes of these regression lines were 0.47 and 0.54 (Table 3). At a significance level of 0.001, we cannot reject the hypothesis that the slope of Model B is equal to 1.0. Of the two valid models, Model B:

$$\log(\text{PDI} + 1) = 1.77 - 0.051S + 0.378C_{pro} - 0.037E_d \quad [10]$$

or:

$$\text{PDI} = 59 \times 0.89^S 2.4^{C_{pro}} 0.92^{E_d} - 1 \quad [11]$$

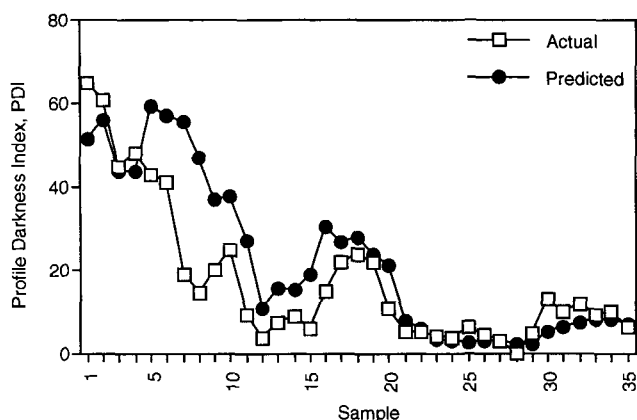


Fig. 6. Actual and predicted Profile Darkness Index (PDI) values along a transect from summit to depression.

has the highest Moran's  $I$   $P$  value (lowest spatial autocorrelation) and the highest validation  $r^2$ . A plot of actual and predicted PDI along a transect from summit to depression (Fig. 6) demonstrates that, in general, the model overpredicts PDI in the lower landscape positions and underpredicts PDI on the upper hillslope. This is also demonstrated by the slopes  $<1$  for the validation data set (Table 3). These results suggest that additional environmental variables, such as the depth to the dense till contact, contribute to the control of water flow over and through the soils of this hillslope. More accurately calculated values of  $A_s$  may also improve model predictions. We used Model B (Eq. [11]) to illustrate and discuss both the applications and limitations of this terrain analysis approach.

An extension of this technique is to apply this model to the entire database of terrain attributes to produce a predictive map of PDI. A plot of PDI across this landscape (Fig. 7a) further illustrates the trend of increasing PDI in the lower landscape positions. This also demonstrates the ability to model the spatial occurrence of PDI using terrain attributes. However, it is important to note that, because samples were only taken from the southwest slope of the study area, the validity of the model across this entire landscape cannot be verified. While a lack of transportability is a potential limitation of any empirical model, our model should be applicable to most other hillslopes in the closed drainage landscapes of the Alexandria Moraine Complex of western Minnesota. In other landscapes, model parameters or model variables will change.

From this direct prediction of PDI we can indirectly estimate the aerial extent of hydric soils across this landscape given the statistical relationship between PDI and the duration of saturated and reducing conditions in the upper 30 cm of the soils at this study site (Thompson and Bell, 1996). By establishing a threshold value for PDI associated with hydric soils on this hillslope (Thompson and Bell, 1996), maps of the spatial distribution of presumed hydromorphic soils can be generated (Fig. 7b). From currently available hydrologic data at five monitoring stations along this hillslope, a PDI value of 29.0 is associated with the soil at the toeslope position and is presumably hydric (piezometric surface within

30 cm of soil surface for  $>2$  wk during the growing season). Soils with lower PDI values were not saturated within the upper 30 cm of the soil (Thompson and Bell, 1996). Further validation of this model is obtained by examining a contingency table for samples above and below the threshold value (Tables 4 and 5). For the (unbiased) validation data set, the model accuracy was 66%. When applied to the entire data set, model accuracy was 81%, although this percentage is biased because 75% of the samples were used to generate the model. The greatest instance of errors in this classification is due to overprediction of PDI, which leads to the misclassification of presumed hydric soils ( $PDI \geq 29$ ) when soil morphology suggests it is nonhydric ( $PDI < 29$ ).

The combination of terrain characteristics associated with high PDI values demonstrates the influence of landscape position and surface geometry on soil morphologies associated with soil saturated conditions. The distributions of terrain attributes above and below the threshold value (Fig. 8) can be used to distinguish between terrain attributes characteristic of presumed hydric and nonhydric soils. The mean attributes of presumed hydric soils ( $PDI \geq 29$ ) are a relatively gentle slope gradient (2.7%), with concave profile curvature, located  $<1.5$  m above the lowest elevation of the local depressional basin (Table 6). This compares with the mean terrain attributes of presumed nonhydric soils ( $PDI < 29$ ): relatively steep slope gradient (7.6%), slightly convex profile curvature, located  $>7.5$  m above the local depression. The differences between the mean terrain attributes of presumed hydric and nonhydric soils (Table 6) are all significant ( $P < 0.001$ ), although differences in the distributions of profile curvature are slight (Fig. 8b). This approach quantifies topographic conditions that may be associated with the occurrence of hydric soils and can be used to establish guidelines to assist wetland professionals with field delineations of hydric soils. For example, the results of our study suggest that in the Alexandria Moraine Complex of central Minnesota, hydric soils are likely to occur on concave slopes with gradients of  $<2$  to 3% that are located  $<1$  to 2 m above a local topographic depression. While this statement may seem intuitive to a pedologist, the articulation of these landscape guidelines are of considerable value to wetland delineators in conceptualizing and estimating the spatial extent of hydric soils. It also forms the linkage between easily observable topographic attributes and the associated variability of soil characteristics, a concept that is obvious to pedologists but requires reinforcement with soil technicians engaged in wetland delineation.

## CONCLUSIONS

This study quantified statistically valid relationships between spatial patterns of terrain attributes and spatial patterns of a color index, PDI, associated with the occurrence of hydric soils in glacial landscapes of west-central Minnesota. Given the relationship between PDI and the duration of saturated and reducing conditions in the

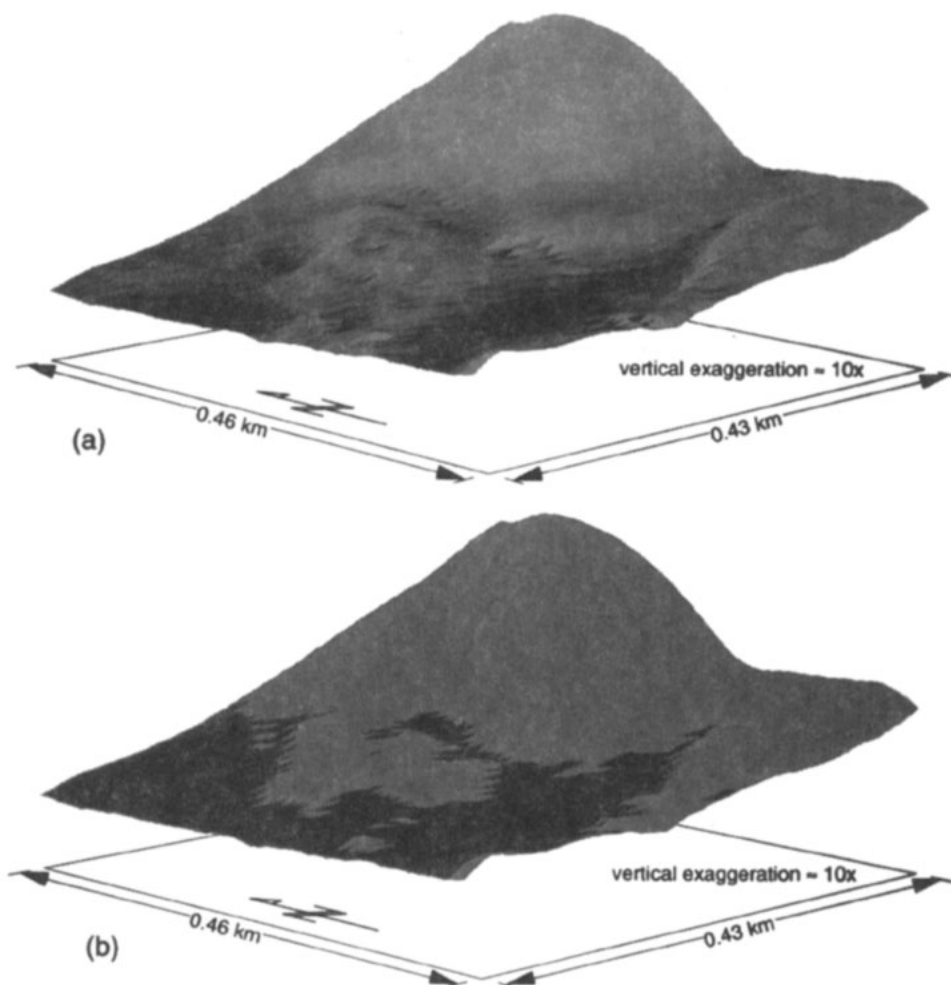


Fig. 7. Drape over study site topography of (a) Profile Darkness Index (PDI), where darker colors indicate higher PDI values, and (b) PDI threshold indicating presumed hydric (black) and nonhydric (gray) soils.

upper 30 cm of the soil, the model predictions of PDI can be used to estimate the spatial distribution of hydric soils. While statistically significant, there is uncertainty in both of these relationships. The PDI explains 48% of the variability in the duration of saturated conditions in the upper 30 cm at 14 pedons in three hillslopes in Minnesota (Thompson and Bell, 1996). At this study site, terrain attributes predict 64% of the variability of PDI in the training data (Table 3). This uncertainty can be viewed as a limitation, but it does allow the possible quantification of this uncertainty associated with the

identification of hydric soils using soil morphological evidence. Only qualitative and semiquantitative relationships are known between other indicators of hydric soil conditions and the duration of saturated conditions (e.g., Veneman et al., 1976; Pickering and Veneman, 1984; Evans and Franzmeier, 1986; Khan and Fenton, 1994), so no level of uncertainty is known.

Specific terrain attributes associated with presumed hydric soils include concave slopes of low (<2–3%) gradient located <1 to 2 m above the lowest elevation of the local topographic depression. The relationship

Table 4. Contingency table for validation data set ( $n = 32$ ) comparing actual and predicted Profile Darkness Index (PDI) values above and below the presumed-hydric soil threshold value of 29 (Thompson and Bell, 1996).

Actual	Predicted		Omission error†	Commission error‡	Accuracy§
	PDI ≥ 29	PDI < 29			
	no.				
PDI > 29	2	1	33	333	67
PDI < 29	10	19	34	3	66
				Overall	66

† Percentage not classified into correct category.

‡ Percentage classified into incorrect category.

§ Percentage classified into correct category.

Table 5. Contingency table for complete data set ( $n = 143$ ) comparing actual and predicted Profile Darkness Index (PDI) values above and below the presumed-hydric soil threshold value of 29 (Thompson and Bell, 1996).

Table 2. (Thompson and Ben, 1978).					
Actual	Predicted		Omission error†	Commission error‡	Accuracy§
	PDI ≥ 29	PDI < 29			
	no.				
PDI > 29	23	9	28	56	72
PDI < 29	18	93	16	8	84
				Overall	81

† Percentage not classified into correct category.

‡ Percentage classified into incorrect category.

§ Percentage classified into correct category.



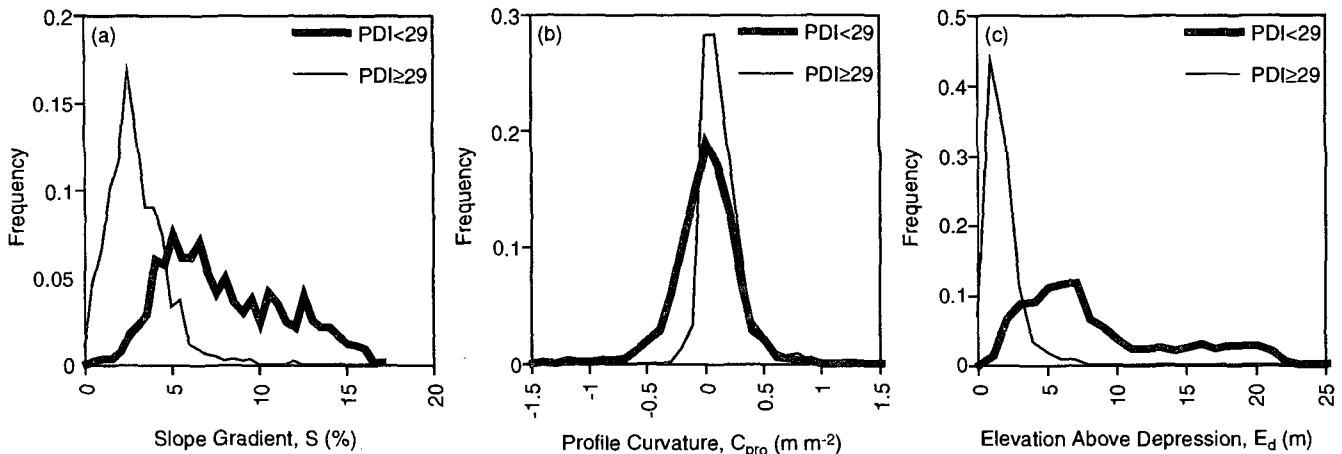


Fig. 8. Histograms for (a) slope gradient,  $S$ ; (b) profile curvature,  $C_{pro}$ ; and (c) elevation above depression,  $E_d$ .

between topography and hydromorphic soil characteristics reinforces the importance of soil hydrology as the primary soil-forming factor affecting the spatial variability of soil characteristics at the hillslope scale. A soil-landscape modeling approach has several advantages including consistent assignment of soil attributes based on observable landscape features, documentation of the decision-making criteria, and creation of a product suitable for use in geographic information systems.

While this study focused on a single hillslope, further development of these models may allow accurate and quantitative mapping of hydromorphic soil characteristics using data derived from digital elevation models of appropriate resolution. Such maps could be useful to field mappers as guides in their own delineation of hydromorphic soils. The advantage of using terrain analysis methods over the interpretation of soil survey data is that it is quantitative and a level of statistical significance can be assigned. However, soil-landscape modeling techniques are not intended to replace the judgment of the field scientist, but rather to enhance the decision-making process and begin to quantify relationships between soil and topographic attributes for environmental modeling purposes.

#### ACKNOWLEDGMENTS

We acknowledge the contributions of Dr. Jim Richardson, Todd Soukup, and Lynn Foss at North Dakota State University for assistance in data collection at this study site. We also acknowledge the contributions of Dr. Warren Lynn (Natural Resources Conservation Service) and Dr. Steve Sprecher (U.S. Corps of Engineers) for leading this research initiative at the national level. Portions of this research were supported

by funds provided by Natural Resources Conservation Service, Corps of Engineers Waterways Experiment Station, the Minnesota Agricultural Experiment Station, and the University of Minnesota Graduate School. We also thank Dr. Dave Grigal and Dr. David Mulla of the University of Minnesota for offering many thoughtful comments that improved this manuscript.

#### REFERENCES

- Bell, J.C., R.L. Cunningham, and M.W. Havens. 1992. Calibration and validation of a soil-landscape model for predicting soil drainage class. *Soil Sci. Soc. Am. J.* 56:1860-1866.
- Bell, J.C., R.L. Cunningham, and M.W. Havens. 1994a. Soil drainage class probability mapping using a soil-landscape model. *Soil Sci. Soc. Am. J.* 58:464-470.
- Bell, J.C., J.A. Thompson, C.A. Butler, and K. McSweeney. 1994b. Modeling soil genesis from a landscape perspective. p. 179-195. *In* Trans. Int. Congr. Soil Sci. 15th, Acapulco, Mexico. 10-17 July 1994. Vol. 6a. ISSS, Vienna.
- Carter, B.J., and E.J. Ciolkosz. 1991. Slope gradient and aspect effects on soils developed from sandstone in Pennsylvania. *Geoderma* 49: 199-213.
- Clark, W.A.V., and P.L. Hosking. 1986. Statistical methods for geographers. John Wiley & Sons, New York.
- Cliff, A.D., and J.K. Ord. 1981. Spatial processes: Models and applications. Pion, London.
- Devore, J., and R. Peck. 1986. Statistics: The exploration and analysis of data. West Publishing Co., St. Paul, MN.
- Donald, R.G., D.W. Anderson, and J.W.B. Stewart. 1993. The distribution of selected soil properties in relation to landscape morphology in forested Gray Luvisol soils. *Can. J. Soil Sci.* 73:165-172.
- Environmental Systems Research Institute. 1987. ARC/INFO users guide. Environ. Syst. Res. Inst., Redlands, CA.
- Evans, C.V., and D.P. Franzmeier. 1986. Saturation, aeration, and color patterns in a toposequence of soils in north-central Indiana. *Soil Sci. Soc. Am. J.* 50:975-980.
- Gessler, P.E., I.D. Moore, N.J. McKenzie, and P.J. Ryan. 1995. Soil-landscape modelling and the spatial prediction of soil attributes. *Int. J. Geogr. Inf. Syst.* 9(4):421-432.
- Jones, J.P., and S.A. Foster. 1991. Testing regression residuals for spatial autocorrelation using SAS: A technical note. *Geogr. Res. Forum* 11:78-83.
- Khan, F.A., and T.E. Fenton. 1994. Saturated zones and soil morphology in a Mollisol catena of central Iowa. *Soil Sci. Soc. Am. J.* 58: 1457-1464.
- Kleiss, H.J. 1970. Hillslope sedimentation and soil formation in north-eastern Iowa. *Soil Sci. Soc. Am. Proc.* 34:287-290.
- Khoros Group. 1991. Khoros users manual. Dep. of Electrical Eng., Univ. of New Mexico, Albuquerque.
- Mader, D.L. 1963. Soil variability: A serious problem in soil site studies in the Northeast. *Soil Sci. Soc. Am. Proc.* 27:707-709.

Table 6. Average values of terrain attributes above and below the Profile Darkness Index (PDI) presumed-hydric soil threshold value of 29 (Thompson and Bell, 1996). Differences in the means are all significant ( $P < 0.001$ ).

	Observations	Slope gradient	Profile curvature	Elevation above depression
	no.	%	m m <sup>-2</sup>	m
PDI < 29	1099	7.6	-0.0487	7.9
PDI ≥ 29	705	2.7	0.108	1.3

- Mausbach, M.J., and J.L. Richardson. 1994. Biogeochemical processes in hydric soil formation. *Curr. Top. Wetland Biogeochem.* 1:68-127.
- Moore, I.D. 1992. Terrain analysis programs for the environmental sciences (TAPES). *Agric. Syst. Inf. Technol.* 4(2):37-39.
- Moore, I.D., P.E. Gessler, G.A. Nielsen, and G.A. Peterson. 1993. Soil attribute prediction using terrain analysis. *Soil Sci. Soc. Am. J.* 57:443-452.
- Moore, I.D., and R.B. Grayson. 1991. Terrain-based catchment partitioning and runoff prediction using vector elevation data. *Water Resour. Res.* 27:1177-1191.
- Moore, I.D., R.B. Grayson, and A.R. Ladson. 1991. Digital terrain modeling: A review of hydrological, geomorphological, and biological applications. *Hydrol. Processes* 5:3-30.
- Moore, I.D., A. Lewis, and J.C. Gallant. 1994. Terrain attributes: Estimation methods and scale effects. p. 189-214 *In* A.J. Jakeman et al. (ed.) *Modelling change in environmental systems*. John Wiley & Sons, London.
- Moore, I.D., E.M. O'Loughlin, and G.J. Burch. 1988. A contour-based topographic model for hydrological and ecological applications. *Earth Surf. Processes Landforms* 13:305-320.
- National Research Council. 1995. *Wetlands: Characteristics and boundaries*. Natl. Academy Press, Washington, DC.
- Neter, J., W. Wasserman, and M.H. Kutner. 1989. *Applied linear regression models*. 2nd ed. Richard D. Irwin, Homewood, IL.
- Odeh, I.O.A., A.B. McBratney, and D.J. Chittleborough. 1994. Spatial prediction of soil properties from landform attributes derived from a digital elevation model. *Geoderma* 63:197-214.
- Odland, J. 1988. *Spatial autocorrelation*. Sage Publ., Newbury Park, CA.
- Oehlert, G.W., and C. Bingham. 1993. *MacAnova user's guide*. Tech. Rep. no. 493. Univ. Minnesota School of Statistics, St. Paul.
- O'Loughlin, E.M. 1986. Prediction of surface saturation zones in natural catchments by topographic analysis. *Water Resour. Res.* 22: 794-804.
- Parker, W.B., S.P. Faulkner, and W.H. Patrick. 1985. Soil wetness and aeration in selected soils with aquic moisture regimes in the Mississippi and Pearl River deltas. p. 91-107. *In* *Wetland soils: Characterization, classification, and utilization*. IRR1, Los Baños, Philippines.
- Pennock, D.J., and E. de Jong. 1990. Regional and catenary variations in properties of Borolls of southern Saskatchewan, Canada. *Soil Sci. Soc. Am. J.* 54:1697-1701.
- Pickering, E.W., and P.L.M. Veneman. 1984. Moisture regimes and morphological characteristics in a hydrosequence in central Massachusetts. *Soil Sci. Soc. Am. J.* 48:113-118.
- Pope, P.T., and J.T. Webster. 1972. The use of an *F*-statistic in stepwise regression procedures. *Technometrics* 14(2):327-340.
- Powell, J.C., and M.S. Springer. 1965. Composition and precision of classification of several mapping units of the Appling, Cecil, and Lloyd series in Walton County, Georgia. *Soil Sci. Soc. Am. Proc.* 29:454-458.
- Royle, A.G., F.L. Clausen, and P. Frederiksen. 1981. Practical universal kriging and automatic contouring. *Geoprocessing* 1:377-394.
- Ruhe, R.V. 1975. *Geomorphology*. Houghton Mifflin, Boston.
- Ruhe, R.V., and P.H. Walker. 1968. Hillslope models and soil formation: I. Open systems. p. 551-560. *In* *Trans. Int. Congr. Soil Sci.* 9th, Adelaide. 1968. Vol. 4. Elsevier, New York.
- Soil Survey Division Staff. 1993. *Soil survey manual*. USDA-SCS Agric. Handb. no. 18. U.S. Gov. Print. Office, Washington, DC.
- Stolt, M.H., and J.C. Baker. 1995. Evaluation of National Wetland Inventory maps to inventory wetlands in the southern Blue Ridge of Virginia. *Wetlands* 15(4):346-353.
- SYSTAT. 1992. *SYSTAT: Statistics*. Version 5.2 ed. SYSTAT, Evanston, IL.
- Thompson, J.A., and J.C. Bell. 1996. Color index for identifying hydric conditions for seasonally saturated Mollisols in Minnesota. *Soil Sci. Soc. Am. J.* 60:1979-1988.
- Veneman, P.L.M., M.J. Vepraskas, and J. Bouma. 1976. The physical significance of soil mottling in a Wisconsin toposequence. *Geoderma* 15:103-118.
- Walker, P.H., and R.V. Ruhe. 1968. Hillslope models and soil formation: I. Closed systems. p. 561-568. *In* *Trans. Int. Congr. Soil Sci.* 9th, Adelaide. 1968. Vol. 4. Elsevier, New York.
- Wilding, L.P., R.B. Jones, and G.M. Schafer. 1965. Variation of soil morphological properties within Miami, Celina, and Crosby mapping units in west-central Ohio. *Soil Sci. Soc. Am. Proc.* 29:711-717.
- Wilding, L.P., G.M. Schafer, and R.B. Jones. 1964. Morley and Blount soils: A statistical summary of certain physical and chemical properties of some selected profiles from Ohio. *Soil Sci. Soc. Am. Proc.* 28:674-679.